

Research Article

A View of Banhatti and Revan Indices in Chemical Graphs

Abid Mahboob,¹ G. Muhiuddin ,² Imran Siddique ,³ and Sajid Mahboob Alam⁴

¹Department of Mathematics, Division of Science and Technology, University of Education, Lahore, Pakistan

²Department of Mathematics, Faculty of Science, University of Tabuk, P. O. Box 741, Tabuk 71491, Saudi Arabia

³Department of Mathematics, University of Management and Technology, Lahore 54770, Pakistan

⁴School of Mathematics, Minhaj University, Lahore, Pakistan

Correspondence should be addressed to G. Muhiuddin; chishtygm@gmail.com and Imran Siddique; imransmsrazi@gmail.com

Received 15 April 2022; Revised 19 May 2022; Accepted 13 June 2022; Published 31 July 2022

Academic Editor: Hassan Raza

Copyright © 2022 Abid Mahboob et al. This is an open access article distributed under the Creative Commons Attribution License, which permits unrestricted use, distribution, and reproduction in any medium, provided the original work is properly cited.

A special type of graph invariant called topological index is the collection of data on algebraic graphs and provides a mathematical way to understand chemical structural features. One of the driving factors behind the wide public attention according to these indices is their remarkable ability to correlate and predict the properties of a wide range of molecular species. Our concern is basically with the study of molecular structures, its shapes, geometries, number of atoms, vertices, bond length, and bond strength. It is very expensive to find the properties of compounds in laboratories due to different expensive apparatus and expensive rare material. It is also time consuming and requires an expert person to perform the experiments. So with the help of graphs and topological index, we want to give an easy approach to find the different characteristics of molecular structures with practical lab experiments. It is a mathematical and theoretical method to estimate the physicochemical properties. Many physicochemical features of a molecular compound can be predicted using topological indices. In this article, we will determine some topological invariants of silicon carbide $\text{SiC}_3\text{-I}[t, u]$ for all values of t and u .

1. Introduction

Chemical graph theory is a field of mathematical chemistry that has a significant impact on the advancement of the chemical sciences. Physicochemical aspects of chemical compounds are frequently characterized in chemical science using molecular-based structural descriptors, also known as graph indices or topological indices; see [1, 2] for graph indices. A chemical graph is a graph in which chemical bonds are portrayed as edges and atoms of a molecule and are portrayed as vertices.

Chemical theory is a branch of graph theory concerned with the discovery of topological indices of chemical graphs that are closely correlated with the chemical properties of chemical compounds. A topological index is a statistical indicator constructed empirically from the network structure. Topological indices have been proven to be effective for assessing correlations between the structure of a molecular compound and its physical characteristics or bioactivities [3–10]. Topological indices are a practical way to convert

chemical composition into numerical values that can be utilized in QSPR and QSAR (quantitative-structure property relationship and quantitative-structure activity relationship, respectively) studies to correlate with physical attributes.

In recent years, the application of graph invariant in QSPR and QSAR investigations has piqued desire. The study of topological indices is extremely important in nanotechnology and theoretical chemistry. Topological indices have been used in chemistry, physics, mathematics, informatics, biology, and other fields [11, 12]. Many topological descriptors were introduced in the latter decades of the 20th century to meet the needs of chemists [13, 14].

The structure utilized in this manuscript is a special isomer of silicon carbide. Silicon carbide has a tetrahedral structure. It is an important gradient for host-guest reaction. It is used in bullet proof jackets, car breaks, LED lights, jewelry, and detectors. Revan and Banhatti indices have a very good correlation with many properties of $\text{SiC}_3\text{-I}[t, u]$.

Kulli is an Indian mathematician who proposed the Banhatti indices by inspiring the Zagreb indices given by

Milan Randic in 1972. Kulli proposed a series of papers on Banhatti indices and gave their different approaches like modified and hyper-Banhatti indices. These indices give excellent correlation with the characteristics of different chemical and nonchemical graphs.

These indices are also helpful in the field of fuzzy mathematics for the study of derived networks [15, 16]. A digital world cannot be imagined without silicon. The discovery of silicon is the great revolution in electronics. Zhao and Zahid explored the structure of silicon with the help of Banhatti and Revan indices [17]. Kulli proposed many papers to study oxide networks, honeycomb networks, drugs, and antibiotic structures with the help of Revan and Banhatti indices [18–20].

1.1. Basic Definitions. In this paper, we indicate a simple connected graph by Γ . The shortest distance between ω and ν is $\mathfrak{B}(\omega, \nu)$. The degree of a vertex ω in graph Γ is denoted by $\mathfrak{B}(\omega)$, an edge between the vertices ω and ν is denoted by $e = \omega\nu$, and the degree of an edge “e” is denoted by $\mathfrak{B}(e)$, where $\mathfrak{B}(e) = \mathfrak{B}(\omega) + \mathfrak{B}(\nu) - 2$ and the maximum and minimum degree in a graph is represented by $\mathfrak{B}(\Gamma)$ and $\delta(\Gamma)$.

We discuss some definitions, and then by utilizing these definitions we can calculate the values of topological indices.

Kulli et al. introduced the first k-Banhatti index $B_1(\Gamma)$ and second k-Banhatti index $B_2(\Gamma)$ in 2016 [21], mathematically defined as follows:

$$B_1(\Gamma) = \sum_{\omega\nu \in E(\Gamma)} [\mathfrak{B}(\omega) + \mathfrak{B}(\nu)],$$

$$B_2(\Gamma) = \sum_{\omega\nu \in E(\Gamma)} [\mathfrak{B}(\omega) \times \mathfrak{B}(\nu)].$$

(1)

In 2020, Kulli checked out the correlation coefficient for chloroquine and hydroxylchloroquine that is used in the pharmaceutical treatment of coronavirus disease 2019. So he mathematically gave the solution to the problem without doing any experiment in the lab. He just deeply studies the structure of medicine and gives information about it by using the Banhatti index [22]. It is the beauty of TIs that we can mathematically estimate the solution to a problem in any field related to graphs or molecular structure. Kulli et al. defined the modified form of first k-Banhatti index ${}^m B_1(\Gamma)$ and second k-Banhatti index ${}^m B_2(\Gamma)$ in 2018 [23]. Mathematically, these are determined as follows:

$${}^m B_1(\Gamma) = \sum_{\omega\nu \in E(\Gamma)} \frac{1}{\mathfrak{B}(\omega) + \mathfrak{B}(e)},$$

$${}^m B_2(\Gamma) = \sum_{\omega\nu \in E(\Gamma)} \frac{1}{\mathfrak{B}(\omega) \times \mathfrak{B}(e)}.$$

(2)

Tang and Abid utilize these indices to discuss molecular networks [24].

In 2016, Kulli [25] proposed first k-hyper-Banhatti index $\eta B_1(\Gamma)$ and second k-hyper-Banhatti index $\eta B_2(\Gamma)$ and are defined as follows:

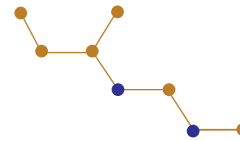


FIGURE 1: Unit cell of $\text{SiC}_3\text{-I}[t, u]$.

$$\eta B_1(\Gamma) = \sum_{\omega\nu \in E(\Gamma)} [\mathfrak{B}(\omega) + \mathfrak{B}(\nu)]^2$$

$$\eta B_2(\Gamma) = \sum_{\omega\nu \in E(\Gamma)} [\mathfrak{B}(\omega) \times \mathfrak{B}(\nu)]^2$$

(3)

Recently in 2021, Zhao and Zahid give the comparison of Banhatti index, Revan index, and hyperindices for the silicon carbide.

In 2017 Kulli [26] proposed first hyper-Revan indices $\eta \hat{R}_1(\Gamma)$ and second hyper-Revan indices $\eta \hat{R}_2(\Gamma)$ and are defined as follows:

$$\eta \hat{R}_1(\Gamma) = \sum_{\omega\nu \in E(\Gamma)} [r_\Gamma(\omega) + r_\Gamma(\nu)]^2$$

$$\eta \hat{R}_2(\Gamma) = \sum_{\omega\nu \in E(\Gamma)} [r_\Gamma(\omega) \times r_\Gamma(\nu)]^2.$$

(4)

The first Revan vertex index and third Revan index of a graph Γ can be defined as follows:

$$\hat{R}_1(\Gamma) = \sum_{\omega\nu \in E} r_\Gamma(\omega)^2$$

$$\hat{R}_3(\Gamma) = \sum_{\omega\nu \in E} |r_\Gamma(\omega) - r_\Gamma(\nu)|,$$

(5)

where $r_\Gamma(\omega) = \mathfrak{B}(\Gamma) + \delta(\Gamma) - \mathfrak{B}(e)$ and $\omega\nu$ means that the vertex ω and vertex ν are adjacent in Γ . We calculate $B_1(\Gamma)$, $B_2(\Gamma)$, ${}^m B_1(\Gamma)$, ${}^m B_2(\Gamma)$, $\eta B_1(\Gamma)$, $\eta B_2(\Gamma)$, $\eta \hat{R}_1(\Gamma)$, $\eta \hat{R}_2(\Gamma)$, $\hat{R}_1(\Gamma)$, and $\hat{R}_3(\Gamma)$ of the nanostructure silicon carbide $\text{SiC}_3\text{-I}[t, u]$.

1.2. 2D Silicon Carbide $\text{Si}_2\text{C}_3\text{-I}[t, u]$. Silicon carbide, commonly referred to as carborundum, is a semiconductor. Silicones are semiconductors that are used in the assembly of a variety of materials. It is an organism that is found in almost all of today’s electrical devices. Silicon, like carbon, has a two-dimensional allotrope with a honeycomb pattern, abbreviated as silicone. Untainted 2D carbon monolayer-graphene, untainted 2D silicon monolayer-silicon, and 2D silicon-carbon (SiC) monolayer can be considered as a tuneable compound. A great deal of effort have gone into predicting the most stable configurations of the SiC sheet. The cardinality of a vertex set $\text{SiC}_3\text{-I}[t, u]$ is $8tu$ and the cardinality of an edge set is $12tu - 2t - 3u$. To construct the topological indices for this chemical composition, we divide the vertex set and edge set into subdivisions. Let $t, u \geq 1$. The vertex is divided into three groups that relying on the vertices of the degree. Graphical representation of 2D silicon-carbide $\text{SiC}_3\text{-I}[t, u]$ is shown in Figures 1–4.

1.3. Edge Partition. The silicon carbide structure has five different sets of edges. The first division of edges consist of just two edges $\omega\nu$, where $\mathfrak{D}(\omega) = 1$ and $\mathfrak{D}(\nu) = 2$. The second

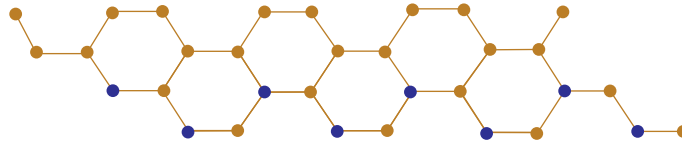


FIGURE 2: $\text{SiC}_3\text{-I}[t, u]$ for $t = 3$ and $u = 1$.

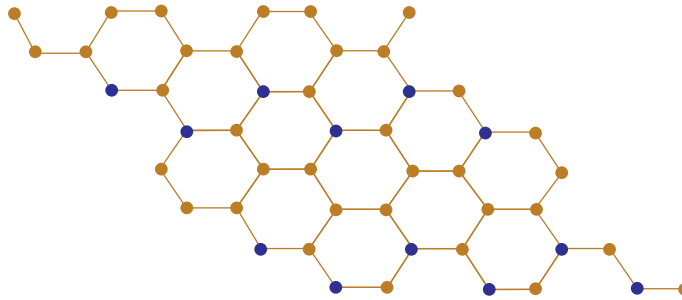


FIGURE 3: $\text{SiC}_3\text{-I}[t, u]$ for $t = 3$ and $u = 2$.

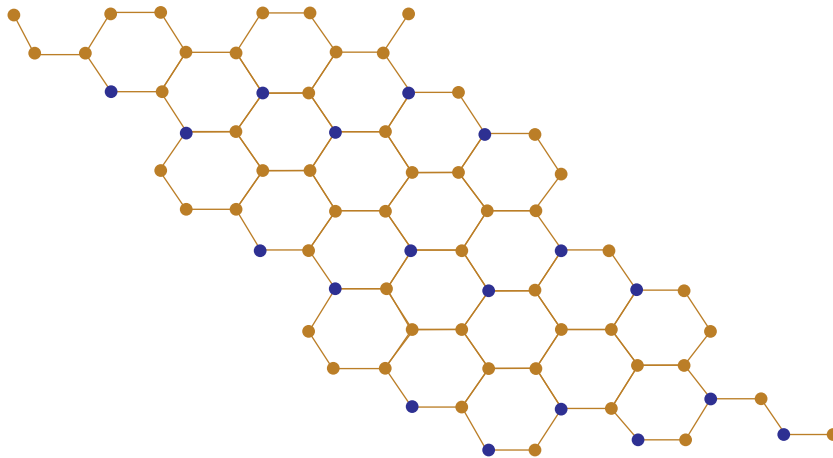


FIGURE 4: $\text{SiC}_3\text{-I}[t, u]$ for $t = 3$ and $u = 3$.

type of set is composed of one edge ωv , where $\bar{d}(\omega) = 1$ and $\bar{d}(v) = 3$. There are $3t + 2u - 3$ edges in the third pack of edges ωv , where $\bar{d}(\omega) = \bar{d}(v) = 2$. The fourth set of edges have $4t + 8u - 8$ edges ωv , where $\bar{d}(\omega) = 3$ and $\bar{d}(v) = 2$. The fifth parcel of edges is made up of $12tu - 8t - 13u + 8$ edges ωv , where $\bar{d}(\omega) = \bar{d}(v) = 3$. Degrees of these edges are also given in Table 1.

1.4. Vertex Partition. The degree of a vertex is the number of edges attached to a vertex. The vertex division is degree-based and has three types of vertices, as given in Table 2. By utilizing this table, we can find many TIs related to the vertex degree.

1.5. Techniques and Methods. We use various methods to calculate TIs, like combinatorial computation, the neighborhood degree counting technique, the vertex degree method, and the edge partition method. For the generalization and verification of calculations, we utilize Matlab. We use

TABLE 1: Edge partitioning of $\text{SiC}_3\text{-I}[t, u]$.

Edges	$(\bar{d}(\omega), \bar{d}(v))$	Frequency	$\bar{d}(e)$	$r_\Gamma(\omega)$	$r_\Gamma(v)$
E_1	(1, 2)	2	1	3	2
E_2	(1, 3)	1	2	3	1
E_3	(2, 2)	$2t + 2u - 3$	2	2	2
E_4	(3, 2)	$4t + 8u - 8$	3	1	2
E_5	(3, 3)	$12tu - 8t - 13u + 8$	4	1	1

TABLE 2: Division of vertices for $\text{SiC}_3 - I[t, u]$.

$\bar{d}(\omega)$	Total vertices	$r_\Gamma(\omega)$
ω_1	3	3
ω_2	$4t + 6u - 6$	2
ω_3	$8tu - 6u - 4t + 3$	1

Mathematica and Maple for drawing 3D graphs. The ChemSketch is helpful for drawing the chemical graphs of silicon. Special software named SPSS is used for correlation analysis.

For 3D graphing, Graphing Calculator 3D and Math Grapher can also be used.

1.6. Fundamental Computations. In this section, we evaluate our numerical results and graphically show the behavior of all TIs with respect to different values of parameters. We use different techniques to find out our required results.

Theorem 1. Let $\Gamma \cong SiC_3-I [t, u]$ be the silicon carbide graph, then k -B indices can be determined as follows:

$$\begin{aligned}
 B_1(\Gamma) &= 168tu - 52t - 78u + 18 \text{ and} \\
 B_2(\Gamma) &= 288tu - 116t - 284u + 62.
 \end{aligned}
 \tag{6}$$

Proof. Table 1 shows the edge partitioning of $SiC_3 - I [t, u]$ based on edge degrees. The $B_1(\Gamma)$ of Γ is then calculated using Table 1 as follows:

$$\begin{aligned}
 &= 2(36) + 9 + (2t + 2u - 3)(16) + (4t + 8u - 8)(4) \\
 &\quad + (12tu - 8t - 13u + 8) \\
 &= 2[(1 \times 1) + (2 \times 1)] + 2[(1 \times 2) + (3 \times 2)] \\
 &\quad + (2t + 2u - 3)[(2 \times 2) + (2 \times 2)] + (4t + 8u - 8) \\
 &\quad [(3 \times 3) + (2 \times 3)] + (12t - 8t - 13u + 8)[(3 \times 4) + (3 \times 4)] \\
 &= 2(5) + 8 + (2t + 2u - 3)(8) + (4t + 8u - 8)(11) \\
 &\quad + (12tu - 8t - 13u + 8)(14) \\
 &= 10 + 8 + 16t + 16u - 24 + 44t + 88u - 88 + 168tu \\
 &\quad - 112t - 182u + 112 \\
 &= 168tu - 52t - 78u + 18.
 \end{aligned}
 \tag{7}$$

$B_2(\Gamma)$ of Γ is described as follows:

$$\begin{aligned}
 B_2(\Gamma) &= \sum_{e=uv} [B(\omega) \times B(e)] = \sum_{e=uv} [B(\omega) \times B(e) + B(v) \times B(e)] \\
 &= 2[(1 \times 1) + (2 \times 1)] + 1[(1 \times 2) + (3 \times 2)] \\
 &\quad + (2t + 2u - 3)[(2 \times 2) + (2 \times 2)] + (4t + 8u - 8) \\
 &\quad \times \times \times \times \times [(3 \times 3) + (2 \times 3)] + (12t - 8t - 13u + 8) \\
 &\quad [(3 \times 4) + (3 \times 4)] \times \times \times \times \\
 &= 2(3) + 8 + (2t + 2u - 3)(8) + (4t + 8u - 8)(15) \\
 &\quad + (12tu - 8t - 13u + 8)(24) \\
 &= 6 + 8 + 16t + 16u - 24 + 60t + 12u - 120 \\
 &\quad + 288tu - 192t - 312u + 192 \\
 &= 288tu - 116t - 284u + 62.
 \end{aligned}
 \tag{8}$$

□

Theorem 2. Let $\Gamma \cong SiC_3 - I [t, u]$ be the silicon carbide; then,

$$\begin{aligned}
 {}^m B_1(\Gamma) &= \frac{24}{7}tu + \frac{19}{105}t + \frac{23}{105}u + \frac{2068}{525} \text{ and} \\
 {}^m B_2(\Gamma) &= 2tu + \frac{7}{9}t + \frac{19}{18}u + \frac{103}{18}.
 \end{aligned}
 \tag{9}$$

Proof. The ${}^m B_1(\Gamma)$ is calculated using Table 1 as follows:

$$\begin{aligned}
 {}^m B_1(\Gamma) &= \sum_{\omega v} \frac{1}{B(\omega) + B(e)} = \sum_{e=uv} \frac{1}{B(\omega) + B(e)} + \frac{1}{B(v) + B(e)} \\
 &= 2\left[\frac{1}{2} + \frac{1}{3}\right] + 1\left[\left(\frac{1}{3}\right) + \left(\frac{1}{5}\right)\right] + (2t + 2u - 3)\left[\left(\frac{1}{4}\right) + \left(\frac{1}{4}\right)\right] + (4t + 8u - 8)\left[\left(\frac{1}{6}\right) + \left(\frac{1}{5}\right)\right] + (12tu - 8t - 13u + 8)\left[\left(\frac{1}{7}\right) + \left(\frac{1}{7}\right)\right] \\
 &\quad + (12tu - 8t - 13u + 8)\left[\frac{1}{7} + \frac{1}{7}\right] \\
 &= 2\left[\left(\frac{5}{6}\right)\right] + \left[\left(\frac{8}{15}\right)\right] + (2t + 2u - 3)\left[\left(\frac{1}{3}\right)\right] + (4t + 8u - 8)\left[\left(\frac{11}{30}\right)\right] + ((12tu - 8t - 13u + 8))\left[\left(\frac{2}{7}\right)\right] \\
 &\quad + \left(12tu - 8t - 13u + 8\right)\left[\frac{2}{7}\right] \\
 &= \left[\left(\frac{10}{6}\right)\right] + \left[\left(\frac{8}{15}\right)\right] + \left(\frac{2}{2}\right)t + \left(\frac{2}{22}\right)u - \left(\frac{3}{2}\right) + \left(\frac{44}{30}\right)t + \left(\frac{88}{30}\right)u - \left(\frac{88}{30}\right) + \left(\frac{24}{7}\right)tu - \left(\frac{16}{7}\right)t - \left(\frac{26}{7}\right)u + \left(\frac{16}{7}\right) \\
 &= \left[\left(\frac{5}{3}\right)\right] + \left[\frac{8}{15}\right] + t + u - \left(\frac{3}{2}\right) + \left(\frac{22}{15}\right)t + \left(\frac{44}{15}\right)u - \left(\frac{44}{15}\right) + \left(\frac{24}{7}\right)tu - \left(\frac{16}{7}\right)t - \left(\frac{26}{7}\right)u + \left(\frac{16}{7}\right) \\
 &= \left(\frac{24}{7}\right)tu + \left(\frac{19}{105}\right)t + \left(\frac{23}{105}\right)u + \left(\frac{2068}{525}\right).
 \end{aligned}
 \tag{10}$$

(10)

Now, we determine the equation of ${}^{\eta}B_2(\Gamma)$:

$$\begin{aligned}
 {}^{\eta}B_2(\Gamma) &= \sum_{\omega v} \frac{1}{B(\omega) \times B(e)} = \sum_{e=\omega v} \frac{1}{B(\omega) \times B(e)} + \frac{1}{B(v) \times B(e)} \\
 &= 2\left[1 + \left(\frac{1}{2}\right)\right] + 1\left[\left(\frac{1}{2}\right) + \left(\frac{1}{6}\right)\right] + (2t + 2u - 3)\left[\left(\frac{1}{4}\right) + \left(\frac{1}{4}\right)\right] + (4t + 8u - 8)\left[\left(\frac{1}{9}\right) + \left(\frac{1}{6}\right)\right] \\
 &\quad + (12tu - 8t - 13u + 8)\left[\left(\frac{1}{12}\right) + \left(\frac{1}{12}\right)\right] \\
 &= 2\left[\frac{3}{2}\right] + \left[\frac{2}{3}\right] + (2t + 2u - 3)\left[\frac{1}{2}\right] + (4t + 8u - 8)\left[\frac{5}{18}\right] + (12tu - 8t - 13u + 8)\left[\frac{1}{6}\right] \\
 &\quad + (12tu - 8t - 13u + 8)\left[\frac{1}{6}\right] \\
 &= 3 + \left(\frac{2}{3}\right) + t + u - \left(\frac{3}{2}\right) + \left(\frac{10}{9}\right)t + \left(\frac{20}{9}\right)u - \left(\frac{20}{9}\right) + \left(\frac{12}{6}\right)tu - \left(\frac{8}{6}\right)t - \left(\frac{13}{6}\right)u + \left(\frac{8}{6}\right) \\
 &= 2tu + \left(\frac{7}{9}\right)t + \left(\frac{19}{18}\right)u + \left(\frac{103}{18}\right).
 \end{aligned} \tag{11}$$

Theorem 3. Let $\Gamma \cong SiC_3 - I[t, u]$ be the silicon carbide graph; then,

$$\begin{aligned}
 \eta B_1(\Gamma) &= 1176tu - 476t - 722u + 260 \text{ and} \\
 \eta B_2(\Gamma) &= 3456tu - 1772t - 2744u + 1322.
 \end{aligned} \tag{12}$$

Proof. The $\eta B_1(\Gamma)$ is calculated as follows:

$$\begin{aligned}
 \eta B(\Gamma) &= \sum_{e=\omega v} [B(\omega) + B(v)]^2 \\
 &= \sum_{e=\omega v} (B(\omega) + B(e))^2 + (B(v) + B(e))^2 \\
 &= 2\left[(1+1)^2 + (2+1)^2\right] + 1\left[(1+2)^2 + (3+2)^2\right] \\
 &\quad + (2t + 2u - 3)\left[(2+2)^2 + (2+2)^2\right] + \\
 &\quad + (4t + 8u - 8)\left[(3+3)^2 + (2+3)^2\right] + 12tu - 8t - 13u \\
 &\quad + 8\left[(3+4)^2 + (3+4)^2\right] \\
 &= 2(13) + 34 + (2t + 2u - 3)(32) + (4t + 8u - 8)(61) \\
 &\quad + (12tu - 8t - 13u + 8)(98) \\
 &= 26 + 34 + 64t + 64u - 96 + 244t + 488u - 488 \\
 &\quad + 1176tu - 784t - 1274u + 784 \\
 &= 1176tu - 476t - 722u + 260.
 \end{aligned} \tag{13}$$

$\eta B_2(\Gamma)$ is determined as follows:

$$\begin{aligned}
 \eta B_2(\Gamma) &= \sum_{e=\omega v} [B(\omega) \times B(v)]^2 \\
 &= \sum_{e=\omega v} [(B(\omega) \times B(e))^2 + (B(v) \times B(e))^2] \\
 &= 2\left[(1 \times 1)^2 + (2 \times 1)^2\right] + 1\left[(1 \times 2)^2 + (3 \times 2)^2\right] \\
 &\quad + (2t + 2u - 3)\left[(2 \times 2)^2 + (2 \times 2)^2\right] \\
 &\quad + (4t + 8u - 8)\left[(3 \times 3)^2 + (2 \times 3)^2\right] \\
 &\quad + 12tu - 8t - 13u + 8\left[(3 \times 4)^2 + (3 \times 4)^2\right] \\
 &\quad + (4t + 8u - 8)(117) + (12tu - 8t - 13u + 8)(288) \\
 &= 10 + 40 + 64t + 64u - 96 + 468t + 936u \\
 &\quad - 936 + 3456tu - 2304t - 3744u + 2304 \\
 &= 3456tu - 1772t - 2744u + 1322.
 \end{aligned} \tag{14}$$

Theorem 4. Let $\Gamma \cong SiC_3 - I[t, u]$ be the graph of silicon carbide; then,

$$\begin{aligned}
 \eta R_1'(\Gamma) &= 48tu + 36t + 52u - 22 \text{ and} \\
 \eta R_2'(\Gamma) &= 12tu + 40t + 51u + 9.
 \end{aligned} \tag{15}$$

Proof. Let $\Gamma \cong SiC_3 - I[t, u]$ be the graph of silicon carbide. The first hyper-Revans indices $\eta R_1(\Gamma)$ is calculated as follows:

TABLE 3: Numerical analysis of all TIs for $\text{SiC}_3 - I[t, u]$.

Banhatti indices	(t, u) = [1, 1]	(t, u) = [2, 2]	(t, u) = [3, 3]	(t, u) = [4, 4]	(t, u) = [5, 5]
$B_1(\Gamma)$	56	430	1140	2186	3568
$B_2(\Gamma)$,	50	614	1754	3470	5762
${}^m B_1(\Gamma)$	7.76	18.46	36	60.39	91.66
${}^m B_2(\Gamma)$	9.56	17.4	29.23	49.28	64.89
$\eta B_1(\Gamma)$	238	2568	7250	14284	23670
$\eta B_2(\Gamma)$	262	6114	18878	38554	65142
$\eta \dot{R}_1(\Gamma)$	114	346	674	1098	1618
$\eta \dot{R}_2(\Gamma)$	112	239	390	565	764
$\dot{R}_1(\Gamma)$	44	98	168	254	356
$\dot{R}_3(\Gamma)$	8	20	32	44	56

$$\begin{aligned}
 \eta \dot{R}_1(\Gamma) &= \sum_{\omega v \in E} [r_\Gamma(\omega) + r_\Gamma(v)]^2 \\
 &= 2(3+2)^2 + 1(3+1)^2 + (2t+2u-3)(2+2)^2 \\
 &\quad + (4t+8u-8)(1+2)^2 + (12tu-8t-13u+8)(1+1)^2 \\
 &= 2(25) + 16 + (2t+2u-3)(16) + (4t+8u-8)(9) \\
 &\quad + (12tu-8t-13u+8)(4) \\
 &= 50 + 16 + 32t + 32u - 48 + 36t + 72u - 72 + 48tu \\
 &\quad - 32t - 52u + 32 \\
 &= 48tu + 36t + 52u - 22.
 \end{aligned} \tag{16}$$

Second hyper-Revans indices $\eta \dot{R}_2(\Gamma)$ is determined as follows:

$$\begin{aligned}
 \eta \dot{R}_2(\Gamma) &= \sum_{\omega v \in E} [r_\Gamma(\omega) \times r_\Gamma(v)]^2 \\
 &= 2(32)^2 + 1(31)^2 + (2t+2u-3)(22)^2 \\
 &\quad + (4t+8u-8)(12)^2 + 12tu-8t-13u+8(1 \times 1)^2 \\
 &= 2(36) + 9 + (2t+2u-3)(16) + (4t+8u-8)(4) \\
 &\quad + (12tu-8t-13u+8)(1) \\
 &= 72 + 9 + 32t + 32u - 48 + 16t + 32u - 32 + 12tu \\
 &\quad - 8t - 13u + 8 \\
 &= 12tu + 40t + 51u + 9.
 \end{aligned} \tag{17}$$

Theorem 5. Let $\Gamma \cong \text{SiC}_3 - I[t, u]$ be the graph of silicon carbide; then,

$$\begin{aligned}
 \dot{R}_1(\Gamma) &= 8tu + 12t + 18u + 6, \quad \dot{R}_1(\Gamma) = 8tu + 12t + 18u + 6 \text{ and} \\
 \dot{R}_3(\Gamma) &= 4t + 8u - 4.
 \end{aligned} \tag{18}$$

Proof. Let $\Gamma \cong \text{SiC}_3 - I[t, u]$ be the graph of silicon carbide. The first Revan vertex index $\dot{R}_1(\Gamma)$ is calculated as follows:

$$\begin{aligned}
 \dot{R}_1(\Gamma) &= \sum_{\omega v \in E} r_\Gamma(\omega)^2 \\
 &= \sum_{vr_3} [r_\Gamma(\omega^2)] + \sum_{vr_2} [r_\Gamma(\omega^2)] + \sum_{vr_1} [r_\Gamma(\omega^2)] \\
 &= 3(3)^2(4t+6u-6)(2)^2 + (8tu-6t-4u+3)(1)^2 \\
 &= 3(9) + 16t + 24u - 24 + 8tu - 6t - 4u + 3 \\
 &= 27 + 16t + 24u - 24 + 8tu - 6t - 4u + 3 \\
 &= 8tu + 12t + 18u + 6.
 \end{aligned} \tag{19}$$

Moreover, from the definition of $\dot{R}_3(\Gamma)$, we have

$$\begin{aligned}
 \dot{R}_3(\Gamma) &= \sum_{\omega v \in E(G)} |r_\Gamma(\omega) - r_\Gamma(v)| \\
 &= 2(1) + 1(2) + (2t+2u-3)(0) + (4t+8u-8)(1) \\
 &\quad + 12tu-8t-13u+8(0). \\
 &= 2 + 2 + 4t + 8u - 8 \\
 &= 4 + 4t + 8u - 8 \\
 &= 4t + 8u - 4.
 \end{aligned} \tag{20}$$

□

2. Numerical and Graphical Representation

The numerical results of the above calculated topological descriptors for $\text{SiC}_3 - I[t, u]$ are represented in this section. The numerical representation are shown in Table 3. A diagram shows a system of relationships between variable quantities using dots to represent the points of the system or using lines to represent the relations of continuous variables. There are many types of graphs according to the nature of data.

The graphs used in this article are 3D because of two variables. The variation in data can be checked out by just discussing numerical values, but for a clear comparison of different TIs, graphs are the best way. Graphs are easy to understand, and so it clearly saves time, but we must have enough knowledge about variables and slopes to use them. Using various values of t and u , we produced numerical

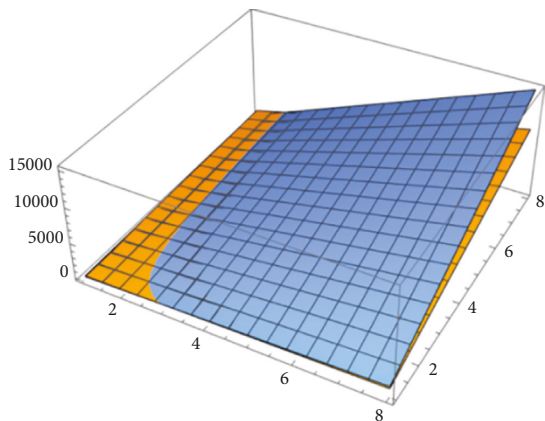


FIGURE 5: $B_1(\Gamma)$ and $B_2(\Gamma)$.

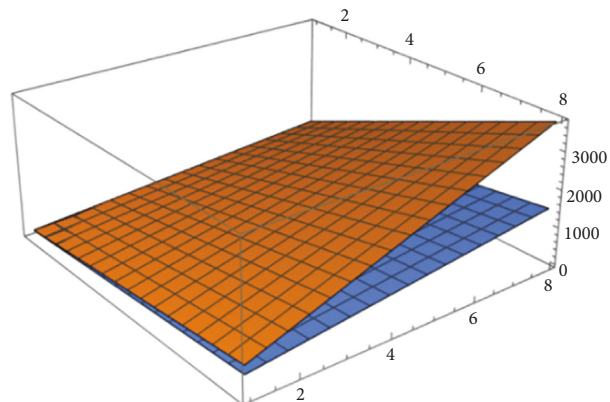


FIGURE 8: $\eta R_1(\Gamma)$ and $\eta R_2(\Gamma)$.

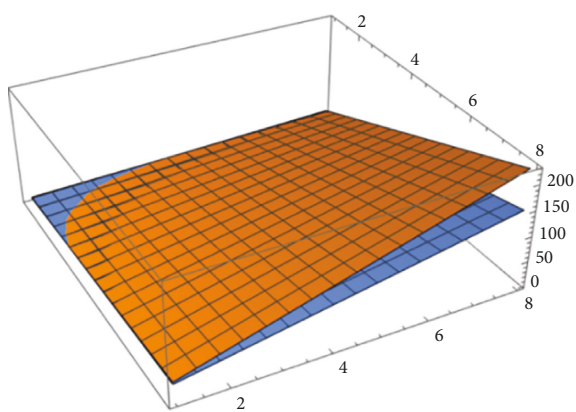


FIGURE 6: $\eta \eta B_1(\Gamma)$ and $\eta \eta B_2(\Gamma)$.

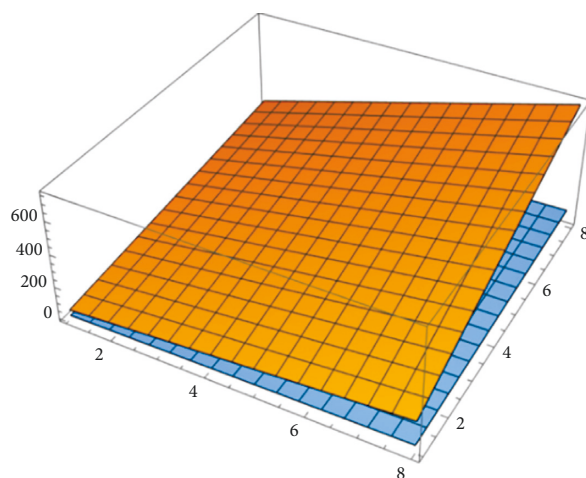


FIGURE 9: $R_1(\Gamma)$ and $R_3(\Gamma)$.

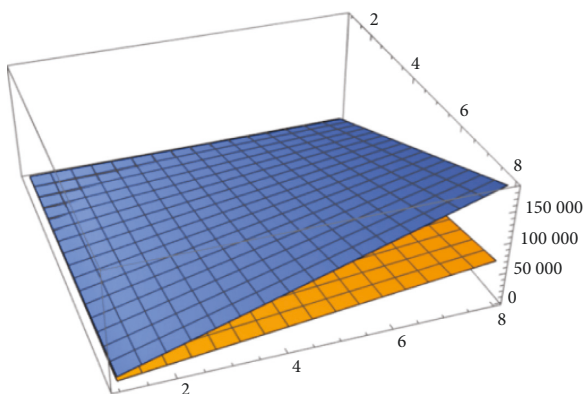


FIGURE 7: $\eta B_1(\Gamma)$ and $\eta B_2(\Gamma)$.

tables/results, as shown in Figures 5–9. The values of all TIs increase when we increase the values of their parameters. The rate of variation of the first and second k-B-index is higher than that of the other TIs. These indices have a correlation with many properties in networking and chemistry. The computed topological descriptors increase in proportion to the rise in t and u .

Graphical representation of above calculated topological indices. These graphs show the variation in the values of TIs with the change of input parameters.

3. Applications

The Banhatti and Revan indices have a very good correlation with different physical and chemical properties of different structures. Asthma drugs are also useful for the treatment of COVID-19. The first Banhatti index has a correlation coefficient $r=0.974$ with molar volume, and the second Banhatti index is correlated with the boiling point ($r=0.9192$) and enthalpy ($r=0.9125$) of these drugs. Hyper-Revan indices are effective to describe the molar volume of asthma drugs. Both these indices have a correlation with the different properties of silicon carbide structures discussed in this manuscript. These indices also tell us about the structural properties of linear alkanes.

4. Conclusion

This analysis delves into the multiplicative and degree-based topological indices for $SiC_3-I [t, u]$. Silicon carbide is a compulsory part of almost every electronic device. Due to the great applications and functions, we try to understand the structure of it. To explore the structure, we applied many indices and saw the correlation of these indices with many important properties of SiC. In this article, we evaluate the

$B_1(\Gamma)$, $B_2(\Gamma)$, ${}^{10}B_1(\Gamma)$, ${}^{10}B_2(\Gamma)$, $\eta B_1(\Gamma)$, $\eta B_2(\Gamma)$, $\eta \hat{R}_1(\Gamma)$, $\eta \hat{R}_2(\Gamma)$, $\hat{R}_1(\Gamma)$, and $\hat{R}_3(\Gamma)$ for Silicon Carbide $SiC_3-I [t, u]$. Our discoveries could assist the understanding of silicon-physical carbon's properties, chemical stability, and bioactivities.

Data Availability

No data were used to support this study.

Conflicts of Interest

The authors declare that they have no conflicts of interest.

References

- [1] V. R. Kulli, "Graph indices," in *Hand Book of Research on Advanced Applications of Application Graph Theory in Modern Society*, M. Pal, S. Samanta, and A. Pal, Eds., pp. 66–91, IGI Global, USA, 2020.
- [2] P. V. Patil and R. Munavalli, "Computing topological indices of certain windmill graphs," *Journal of Computational Mathematics*, vol. 6, no. 1, pp. 001–014, 2022.
- [3] A. Mahboob, S. Mahboob, M. M. M. Jaradat, N. Nigar, and I. Siddique, "On some properties of multiplicative topological indices in silicon-carbon," *Journal of Mathematics*, vol. 2021, pp. 1–10, Article ID 4611199, 2021.
- [4] A. Mahboob, D. Alrowaili, S. M. Alam, R. Ali, M. W. Rasheed, and I. Siddique, "Topological attributes of silicon carbide $SiC_4-II [i, j]$ based on ve-degree and ev-degree," *Journal of Chemistry*, vol. 2022, Article ID 3188993, 2022.
- [5] Z. Q. Cai, A. Rauf, M. Ishtiaq, and M. K. Siddiqui, *On Ve-Degree and Ev-Degree Based Topological Properties of Silicon Carbide $Si_2C_3-II [p, Q]$* , pp. 1–15, Polycyclic Aromatic Compounds, 2020.
- [6] Y. H. Pan, A. Khalid, P. Ali et al., *Topological Study of Polycyclic Silicon Carbide Structure*, pp. 1–12, Polycyclic Aromatic Compounds, 2022.
- [7] M. Arockiaraj, J. B. Liu, M. Arulperumjothi, and S. Prabhu, "On certain topological indices of three-layered single-walled titania nanosheets," *Combinatorial Chemistry & High Throughput Screening*, vol. 25, no. 3, pp. 483–495, 2022.
- [8] A. K. Kn, B. Ns, S. Mc, and S. Kc, "Degree-based topological indices on asthma drugs with QSPR analysis during covid-19," *European Journal of Molecular and Clinical Medicine*, vol. 7, no. 10, pp. 53–66, 2020.
- [9] P. Ali, S. A. K. Kirmani, O. Al Rugaie, and F. Azam, "Degree-based topological indices and polynomials of hyaluronic acid-curcumin conjugates," *Saudi Pharmaceutical Journal*, vol. 28, no. 9, pp. 1093–1100, 2020.
- [10] S. Sorgun, H. Küçük, and K. Birgin, "Some distance-based topological indices of certain polysaccharides," *Journal of Molecular Structure*, vol. 1250, 2022.
- [11] G. Yu, X. Li, and D. He, "Topological indices based on 2-or 3-eccentricity to predict anti-HIV activity," *Applied Mathematics and Computation*, vol. 416, 2022.
- [12] J. B. Liu, "Novel applications of graph theory in chemistry and drug designing," *Combinatorial Chemistry & High Throughput Screening*, vol. 25, no. 3, pp. 439–440, 2022.
- [13] I. Gutman, J. Monsalve, and J. Rada, "A relation between a vertex-degree-based topological index and its energy," *Linear Algebra and Its Applications*, vol. 636, pp. 134–142, 2022.
- [14] Z. S. Mufti, R. Anjum, A. Abbas, S. Ali, M. Afzal, and A. Alam, "Computation of vertex degree-based molecular descriptors of hydrocarbon structure," *Journal of Chemistry*, vol. 2022, pp. 1–15, Article ID 3621403, 2022.
- [15] D. Narasimhan, R. Vignesh, and K. Desikan, "Results on rewan and hyper rewan indices of some HEX derived networks," in *Fuzzy Mathematical Analysis and Advances in Computational Mathematics*, pp. 209–220, Springer, Singapore, 2022.
- [16] W. Gao, B. Muzaffar, and W. Nazeer, "K-Banhatti and K-hyper Banhatti indices of dominating David derived network," *Open J. Math. Anal*, vol. 1(2017), no. 1, pp. 13–24, 2017.
- [17] D. Zhao, M. A. Zahid, R. Irfan et al., "Banhatti, rewan and hyper-indices of silicon carbide $Si_2C_3 -III [n, m]$," *Open Chemistry*, vol. 19, no. 1, pp. 646–652, 2021.
- [18] V. R. Kulli, "Revan indices of oxide and honeycomb networks," *Int. J. Mathematics and its Applications*, vol. 5, no. 4-E, pp. 663–667, 2017.
- [19] V. R. Kulli, "ABC Banhatti and augmented Banhatti indices of chemical networks," *Journal of chemistry and Chemical Sciences*, vol. 8, no. 8, pp. 1018–1025, 2018.
- [20] V. R. Kulli, "K Banhatti polynomials of remdesivir, chloroquine and hydroxychloroquine: research Advances for the prevention and treatment of COVID-19," *SSRG International Journal of Applied Chemistry*, vol. 7, no. 2, pp. 48–55, 2020.
- [21] V. R. Kulli, "On K Banhatti indices of graphs," *Journal of Computer and Mathematical Sciences*, vol. 7, pp. 213–218, 2016.
- [22] K. Vr, "K Banhatti indices of chloroquine and hydroxychloroquine, Research Applied for the treatment and prevention of COVID-19," *International Journal of Applied Chemistry*, vol. 7, no. 1, pp. 63–68, 2020.
- [23] V. R. Kulli, "Computing Banhatti indices of networks," *Int. J. Advan. Math.*, vol. 1, pp. 31–40, 2018.
- [24] J. H. Tang, M. Abid, K. Ali et al., "On computation of edge degree-based banhatti indices of a certain molecular network," *Journal of Mathematics*, vol. 2021, pp. 1–7, 2021.
- [25] V. R. Kulli, "New K-banhatti topological indices," *Int. J. Fuzzy Math. Arch.*, vol. 12, pp. 29–37, 2017.
- [26] V. R. Kulli, "On K hyper Banhatti indices and coindices of graphs," *Int. Res. J. Pure Algrbra*, vol. 6, pp. 300–304, 2016.